Cement & Concrete Composites 32 (2010) 399–410

Contents lists available at ScienceDirect

Cement & Concrete Composites

journal homepage: www.elsevier.com/locate/cemconcomp

Structure and strength of NaOH activated concretes containing fly ash or GGBFS as the sole binder

Deepak Ravikumar, Sulapha Peethamparan, Narayanan Neithalath *

Department of Civil and Environmental Engineering, Clarkson University, Potsdam, NY 13699, USA

ARTICLE INFO

Article history:
Received 10 September 2009
Received in revised form 16 March 2010
Accepted 17 March 2010
Available online 21 March 2010

Keywords:
Microstructure
Compressive strength
Fly ash
Granulated blast furnace slag
Cement-free binder
Porosity
Pore size

ABSTRACT

The influence of the concentration of the activating agent (4, 6, or 8 M sodium hydroxide solution), and activator-to-binder ratio (0.40, 0.50, or 0.60) on the compressive strengths, pore structure features, and microstructure of concretes containing Class F fly ash or ground granulated blast furnace slag (GGBFS) as the sole binder is reported. The starting material contents and the curing parameters (temperature and curing duration) are optimized to provide the highest compressive strengths. Statistical analysis of the compressive strength results show that the activator concentration has a larger influence on the compressive strengths of activated concretes made using fly ash and the activator-to-binder ratio influences the compressive strengths of activated GGBFS concretes to a greater degree. Activated fly ash concretes and pastes are found to be more porous and contains a larger fraction of pores greater than 10 μm in size as compared to activated GGBFS mixtures. The differences in the microstructure and the reaction products between activated fly ash and GGBFS pastes are detailed.

1. Introduction

Increasing emphasis on the environmental impacts of construction materials such as Portland cement has provided immense thrust in recent years to the increased utilization of waste and by-product materials in concretes. Activation of aluminosilicate materials such as fly ash, blast furnace slag, and metakaolin using alkaline solutions to produce binders free of Portland cement is a major advancement towards increasing the beneficial use of industrial waste products and reducing the adverse impacts of cement production. These alkali-activated binder systems appear in the vast available body of literature in a variety of names: alkali-activated cement [1] (predominantly used for binders containing large amounts of calcium such as slags), geopolymer [2–6], inorganic polymer [7], hydroceramic, or low temperature aluminosilicate glass [8]. They are sometimes called polysialates also because of the polymeric silicon–oxygen–aluminum framework [9]. In general, concretes made using alkali activation of the starting aluminosilicate material do not contain Portland cement at all, and hence they are referred to generically as cement-free binder (CFB) concretes in this study. The concretes containing alkali-aluminosilicate gel as the binder has been shown to have high compressive strengths, and resistance to fire, and chemical attack [10–13].

The starting material and activating agent type and concentration are the most important parameters that influence the properties of the alkali-activated end product [14,15]. The production of cement-free binders requires a starting material containing aluminum and silicon species that are soluble in highly alkaline solutions. Previous studies have shown that the amount of vitreous silica and alumina present in the starting material plays a significant role in activation reactions and the properties of the reaction product [10,16]. The presence of calcium oxide in the source material also influences the properties, especially because of the formation of more than one reaction product [17]. Sodium hydroxide and sodium silicate are the more commonly used alkaline activating agents [18–20] even though few studies have also been carried out with potassium hydroxide or sodium carbonate as the activating agent [13,21].

The dissolution stage during alkali activation of aluminosilicates is reported to be similar to that in the hydration of Portland cement at early ages [22,23]. The dissolved species and the active surface groups in the starting material undergo polymerization to form the alkali-aluminosilicate gel with the aluminum cation in fourfold co-ordination with respect to oxygen [24,25] which hardens to form the binder matrix. $M_n[-(SiO_2)_z-AlO_2]_n-wH_2O$ is the general empirical formula proposed for the reaction product formed where M is the alkali ion, usually sodium or potassium, z is 1, 2, or 3, and n is the degree of polymerization [9]. Only a small fraction of the silica and alumina in the source material need to dissolve and participate in the polymerization reaction for the

* Corresponding author. Tel.: +1 315 268 1261; fax: +1 315 268 7985.
E-mail address: nneithal@clarkson.edu (N. Neithalath).

0958-9465/$ - see front matter © 2010 Elsevier Ltd. All rights reserved.
doi:10.1016/j.cemconcomp.2010.03.007

mixture to solidify. The alkali-aluminosilicates produced from fly ash and/or slag to be used as binding materials in concrete are largely X-ray amorphous, attributable to the low alkaline solution-to-starting material ratio. Higher alkaline solution-to-fly ash ratio and longer thermal curing durations have been reported to produce more crystalline reaction products [14,26]. Activation of aluminosilicate materials with alkalis generally requires heat curing for the formation of alkali-aluminosilicates especially when the activating solution does not contain soluble silica. A wide range of temperatures ranging from 40 °C to 90 °C have been reported in order to produce alkali-activated binders with appreciable mechanical properties [18,27–29], with a general improvement in mechanical properties observed when higher temperatures are used.

It has been reported that fly ash and ground granulated blast furnace slag (GGBFS) are very effective as starting materials for cement-free binder concretes because of the soluble silica and alumina contents in these materials that undergo dissolution, polymerization with the alkali, condensation on particle surfaces, and solidification that eventually provides strength and stability to these matrices. This paper focuses on the comparison of CFB concretes and pastes made with fly ash or GGBFS as the starting material, and activated with varying concentrations of sodium hydroxide solution. Since the mechanism of binding gel formation, even with the same activator, is different for both these starting materials, there is a need to understand the effect of activator concentration on the properties of CFB concretes made using different starting materials. The relative influence of the concentration of the alkaline activator and the activator-to-binder ratio on the compressive strengths and porosities of CFB concretes is evaluated in this paper so as to aid in the selection of mixture parameters when either fly ash or GGBFS is used as the starting material. Differences in microstructure (morphology and phase composition) between CFB pastes made with fly ash or GGBFS as the binding material are also brought out in detail.

2. Experimental program

2.1. Starting materials and activator

To prepare CFB pastes and concretes in this study, a Class F fly ash conforming to ASTM C 618 and a ground granulated blast furnace slag (GGBFS) Type 100 conforming to ASTM C 989 were used as the starting materials. The chemical compositions of fly ash and GGBFS are given in Table 1. Both these binding materials are rich in silica and alumina, which are required for the formation of the strength imparting phases in CFB concretes. The silica-to-alumina ratios (SiO_2/Al_2O_3) by mass were found to be approximately 1.75 and 3.41 for fly ash and GGBFS, respectively. Apart from the high silica and alumina contents, GGBFS also has a high CaO content (~40%) while the CaO content in fly ash is very low (5.8%). X-ray diffraction (XRD) patterns of the starting materials are shown in Fig. 1 and the particle size distributions (obtained using a laser particle size analyzer) are shown in Fig. 2. The XRD pattern of fly ash shows a diffuse band corresponding to the glassy phase which peaks at a 2θ of about 23°. For GGBFS, an asymmetric diffuse band of glass is observed between 2θ of 20° and 37°, with the peak at 31°. The XRD patterns show that GGBFS is more amorphous which suggests better reactivity as compared to fly ash which contains crystalline phases of silica and alumina. Particle size analysis shows that GGBFS is finer than fly ash with 95% finer than 30 μm compared to 60% for fly ash, which potentially influences its reactivity. Analytic reagent-grade sodium hydroxide (NaOH) crystals were used to prepare the alkaline activating solutions of varying molar concentrations.

Table 1
Chemical composition and physical characteristics of the starting materials.

Composition/Property	(% by mass)	
	Fly ash (%)	GGBFS (%)
SiO_2	50.2	36.0
Al_2O_3	28.7	10.5
Fe_2O_3	5.72	0.67
CaO	5.86	39.8
MgO	1.74	7.93
Na_2O	0.96[a]	0.27
K_2O		0.16
SO_3	0.51	2.11
Loss on ignition (LOI)	2.80	3.00
Fineness (% finer than 30 μm)	60	95

[a] Equivalent alkalis.

2.2. Mixing procedure

Prior to the preparation of the concrete mixture, NaOH solutions of the desired concentrations were prepared and allowed to stay at room temperature for 2 h. The mixing procedure involved initial mixing of the source material (fly ash or GGBFS), fine aggregate, and the coarse aggregate (nominal maximum size of 9.5 mm) for 2 min. NaOH solution of the desired concentration was then added, and mixed for further 4 min for CFB concretes with fly ash and 2 min for CFB concretes with GGBFS to obtain a uniform mixture. The reason for using only 2 min of mixing for the GGBFS mixtures was the faster rate of setting of NaOH activated GGBFS. The mixtures were then filled in cubical molds of 50 mm size and vibrated by placing on a table vibrator until proper compaction was achieved. GGBFS mixtures were vibrated for 2 min as opposed to fly ash mixtures which needed only 1 min of vibration to achieve adequate compaction. For the paste specimens to be used for microstructural analysis, samples were prepared by mixing the activating solution and the binder in a blender for 2 min. Both the paste and concrete specimens were removed from the molds after 24 h and subjected to heat curing in a laboratory oven at either 60 °C or 75 °C for 24 h or 48 h.

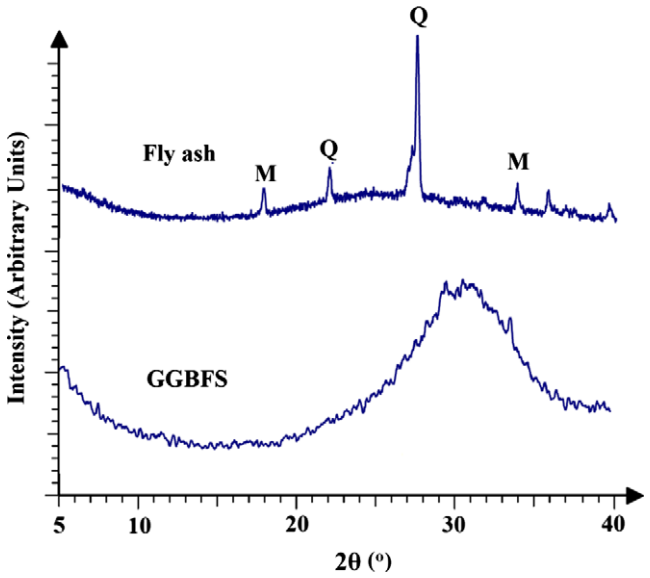

Fig. 1. X-ray diffractions patterns of fly ash and GGBFS powder (Q: quartz, M: mullite).

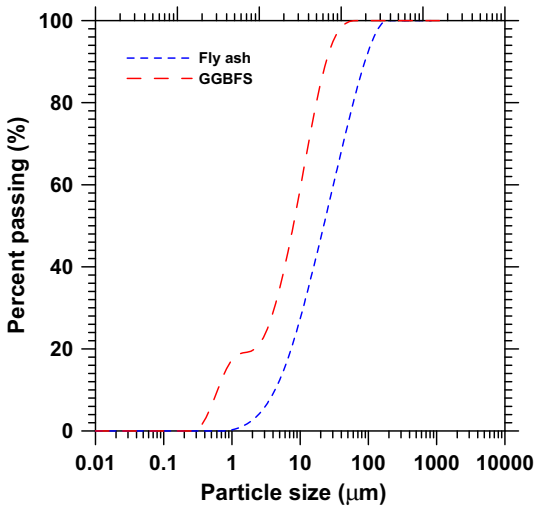

Fig. 2. Particle size distribution of fly ash and GGBFS.

2.3. Determination of optimal binder contents and mixture proportions

In order to obtain the binding material content (by volume) that provides the highest compressive strength for the experimental conditions used, CFB concretes were proportioned using fly ash and GGBFS contents ranging from 15% to 30% by volume of concrete. The coarse aggregate to fine aggregate ratio by mass was approximately 1.1 for all the concrete mixtures. NaOH solution of 8 M concentration (prepared by dissolving 320 g of NaOH in 1 l of water) was used as the activating agent at an activator-to-binder mass ratio of 0.40. The specimens were heat cured at 75 °C for 48 h in a laboratory oven after demolding at 24 h. Fig. 3 shows the compressive strengths of the CFB concretes as a function of either fly ash or GGBFS contents. It can be seen that 18% fly ash content by volume and 25% GGBFS content by volume of the concrete mixture, respectively provided the maximum compressive strengths in this study. These volume fractions of the starting materials were used to proportion concretes for further experiments with different alkali activator concentrations and activator-to-binder ratios. The total aggregate volume in the CFB concretes ranged from 65% to 70% for CFB concretes with fly ash as binder and 55–60% for CFB concretes with GGBFS as binder. The fly ash content ranged from 430 to 445 kg/m^3 and the GGBFS content ranged from 545 to 575 kg/m^3 for the different CFB concrete mixtures. CFB concretes were proportioned using the above determined starting material contents, activator concentrations of 4 M, 6 M, and 8 M NaOH, and activator-to-binder ratios of 0.40, 0.50, and 0.60, to understand the influence of these parameters on the compressive strength. A total of 18 concrete mixtures were proportioned in this study.

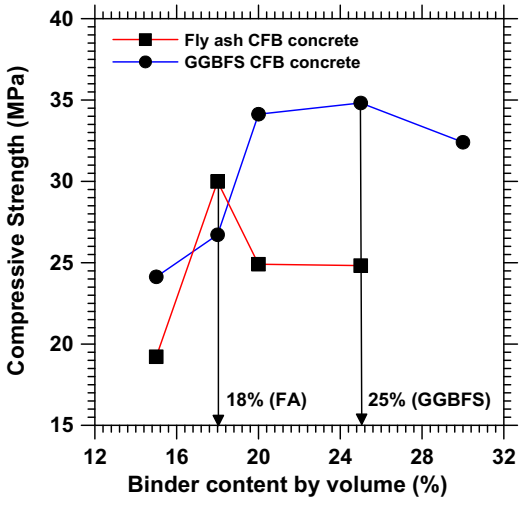

Fig. 3. Determination of optimum starting material content for CFB concretes.

2.4. Determination of strength, porosity, and pore sizes

After the heat curing duration, the concretes were allowed to cool down and return to ambient temperatures. The compressive strengths of the cubes were then determined in accordance with ASTM C 109. No moist curing was adopted for any of the mixtures after the heat curing procedure.

2.4.1. Porosity from vacuum saturation method

The porosities of the CFB concretes and pastes were measured in accordance with the procedure described in RILEM CPC 11.3 [30]. The 50 mm size CFB concrete or paste cubes were cut into two equal halves after the heat curing duration. After measuring the initial mass, the specimens were vacuum dried for 3 h and subsequently saturated under vacuum for 1 h. The specimens were kept submerged in water for a further 18 h after which they were removed from water, surface dried, and weighed. The increase in the mass of the specimen, represented as percentage of the volume of the specimen, is reported as the porosity.

2.4.2. Porosity and pore size of CFB pastes from image analysis

Image analysis technique was used to determine the porosity and pore size distribution of CFB pastes. The cut surfaces of CFB pastes were polished and divided into grids of 3 mm × 3 mm size. Optical microscope was used to capture images of these grids at a magnification of 20. A commercial image analysis and processing software was used to extract the pore structure features. The captured color images were converted to grayscale images, and thresholded to obtain binary images in which the solid (white) and pore (black) areas are clearly differentiated as shown in Fig. 4a and b. The sizes of all the images were 400 pixels × 400 pixels (1 pixel = 3/400 mm). Fig. 4a shows a binary image from a typical CFB paste containing fly ash as the starting material, and Fig. 4b shows the image of a typical paste containing GGBFS as the starting material. The pore area fractions (porosity) of these images were obtained from the image analysis program. The frequency distributions of the pore sizes (assuming the features to be circular in shape) were also obtained for each image. The minimum pore size detected by the optical microscopy procedure was approximately 10 μm. A typical cumulative frequency distribution plot is shown in Fig. 4c. The pore size corresponding to 50% of the cumulative frequency distribution plot is taken as the characteristic size of the pores greater than 10 μm ($d_{50(>10\ \mu m)}$).

2.5. Microstructural analysis

To understand the morphology and the composition of the reaction products formed in NaOH activated CFB pastes, morphological analysis was performed using scanning electron microscopy (SEM) coupled with energy dispersive X-ray analysis (EDX) for elemental composition analysis. X-ray diffraction (XRD) was used to determine the phase composition of the reaction products. The XRD patterns of the powdered paste samples were recorded using a Bruker DX-8 diffractometer. Cu Kα radiation (λ = 1.504 Å) was used and the tests were carried out in the 2θ range of 5–40°, with a step size of 0.02° and step time of 2 s.

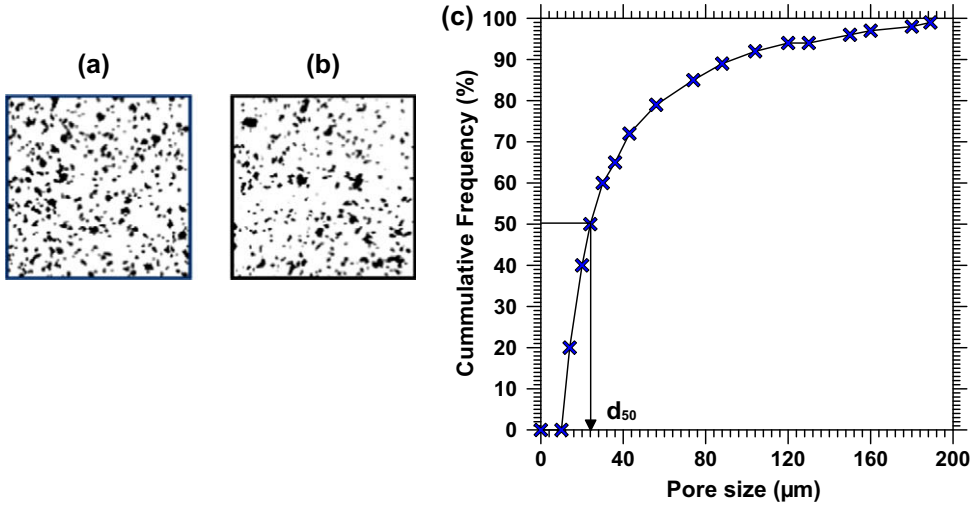

Fig. 4. (a) Binary image for CFB paste with fly ash, (b) binary image of CFB paste with GGBFS, and (c) a typical cumulative frequency distribution plot of pore sizes.

3. Results, analysis, and discussion

3.1. Compressive strength of CFB concretes as functions of curing temperature and duration

Heat curing is required to achieve adequate mechanical properties for CFB concretes activated using NaOH. In order to obtain the curing temperature and duration that provides the maximum compressive strengths, CFB concretes made using an activator-to-binder ratio of 0.40, containing the optimal fly ash or GGBFS contents (18% or 25% by volume, respectively), and activated using 8 M NaOH solution were subjected to temperatures of 60 °C and 75 °C for 12, 24 or 48 h. Fig. 5a and b show the compressive strengths of CFB concretes made using fly ash or GGBFS as the starting materials respectively, as functions of both curing temperature and curing duration. The compressive strengths reported are those determined at the end of the respective curing durations. The poly-condensation of the aluminosilicate gel is likely to continue even after this duration, and strength improvements might occur, especially for mixtures that contain GGBFS as the starting material because of the transformation of metastable amorphous gel to more stable crystalline phases [3]. However, this paper does not consider the above aspect and the compressive strengths of fly ash and GGBFS CFB concretes are compared at the end of the respective curing durations.

Increasing the curing duration from 12 h to 48 h increased the compressive strengths significantly in all the cases as seen from Fig. 5. As observed from Fig. 5a, curing at 60 °C did not produce appreciable compressive strengths for CFB concretes made with fly ash as the starting material, irrespective of the curing duration. Increasing the curing temperature to 75 °C resulted in significant improvements in compressive strengths for these concretes. This point to the fact that a curing temperature of 75 °C is necessary to produce sufficient amounts of sodium aluminosilicate gel necessary to impart strength to CFB concretes containing fly ash. While a curing temperature greater than 75 °C is expected to further increase the strength [26], such an attempt is not made in this study considering the even higher energy requirements.

From Fig. 5b, it can be seen that for CFB concretes made using GGBFS as the starting material, heat curing for 48 h at 60 °C produces appreciable compressive strengths, even though they are lower than those cured at 75 °C for the same duration. The difference in compressive strengths between the specimens heat cured at 60 °C or 75 °C is not as distinct for CFB concretes made using GGBFS as that for those made using fly ash, especially at longer curing durations. This is indicative of the influence of processing

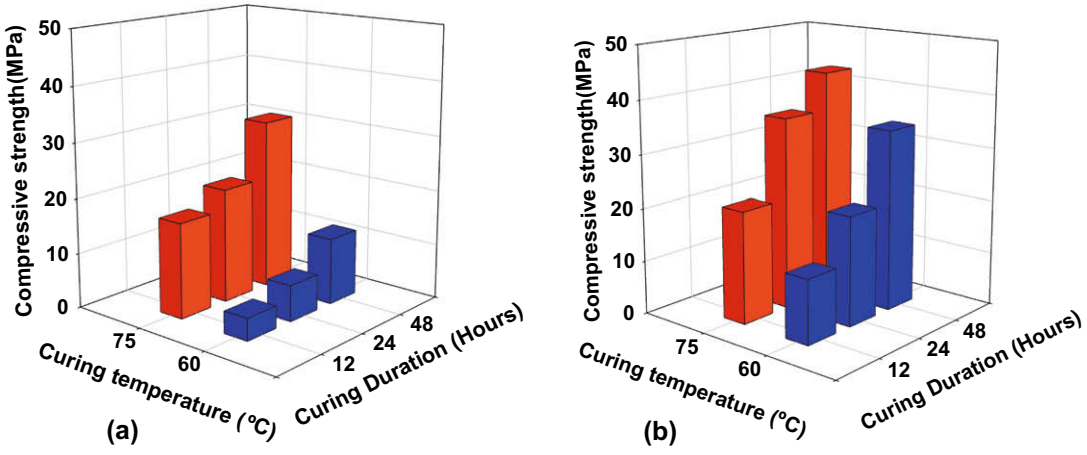

Fig. 5. Influence of curing temperatures and durations on the compressive strengths of CFB concretes with: (a) fly ash, and (b) GGBFS as the starting material.

conditions on the amount and structure of the reaction product (alkali-aluminosilicate gel) in CFB concretes made using fly ash or GGBFS as the starting material. While the presence of calcium oxide in GGBFS would have facilitated the formation of some calcium bearing strength giving components even at lower temperatures, the strength development of CFB concretes made with fly ash is solely dependent on the formation of sodium aluminosilicate gel. Based on these observations, the results reported further in this paper are for specimens (both concretes and pastes) heat cured at 75 °C for 48 h, since this combination of curing temperature and duration provided the highest compressive strengths.

3.2. Dependence of compressive strengths of CFB concretes on activator-to-binder ratios and molar concentration of NaOH

The influence of activator-to-binder ratios and molar concentrations of NaOH on the compressive strengths of CFB concretes containing fly ash or GGBFS are shown in Fig. 6a and b, respectively. These figures show that the compressive strengths increase with increase in the molar concentration of NaOH used as the activator.

Compressive strengths are found to decrease with increase in activator-to-binder ratio even though a higher activator-to-binder ratio effectively contains a higher amount of the activating alkali. This shows that the higher porosity created because of the increased amounts of the activating solution, and the substantial increase in number of pores greater than 10 μm as result of curing in dry heat (stated in [31], and experimentally shown later in this paper) are more prominent than the effect of increased NaOH concentration (that potentially could produce increased amounts of reaction product) on the compressive strength in the range of activator concentrations and activator-to-binder ratios used in this study. A closer look at these figures also indicates that the strength drop with increasing activator-to-binder ratio is greater for CFB concretes made with GGBFS as the starting material. This might be due to the increased capillary porosity created in the cementitious material hydration product because of the increase in activator-to-binder ratio.

The activation of GGBFS with NaOH produced concretes of higher compressive strengths than those produced by the activation of fly ash. The higher reactivity and self-cementing property of GGBFS could partly be the reason for the higher compressive strengths of CFB concretes made using GGBFS. It needs to be also remembered that a higher volume of GGBFS could be incorporated into the CFB concrete mixtures for maximum compressive strength, thereby contributing to a portion of the increased strength. As could be observed from Fig. 3, the binder contents were chosen so as to maximize the compressive strengths of CFB concretes using fly ash and GGBFS as the binder, and not on obtaining identical strengths.

For CFB concretes made with fly ash as the starting material, the compressive strengths obtained by activation using 4 M and 6 M NaOH were low and almost similar, and activation with 8 M NaOH resulted in increased compressive strengths, pointing to insufficient activation of fly ash at low concentrations of the activator. For CFB concretes with GGBFS as the starting material, Fig. 6b shows that activation with lower concentrations of NaOH (4 M and 6 M) also provided reasonable compressive strengths unlike CFB concretes with fly ash. The relatively lower difference in strengths between CFB concretes made using GGBFS activated by either 6 M or 8 M NaOH as compared to that of CFB concretes with fly ash is evidence of the relatively lesser influence of activator concentration (within the ranges studied) when GGBFS is used as the starting material.

Since the optimum binder contents for CFB concretes made with GGBFS as the starting material were higher than those for CFB concretes made with fly ash, the compressive strengths of different CFB concretes cannot be compared directly. Hence the measured compressive strengths were normalized by the binder content used in the particular mixture. Fig. 7a and b shows the normalized compressive strengths for CFB concretes made using fly ash and GGBFS respectively as the starting material. It can be immediately noticed from these figures that, at higher activator concentrations, the CFB concretes show very similar strengths per unit binder content irrespective of the binder type and the activator-to-binder ratio. This is an indication of better utilization of fly ash particles in forming the reaction product when higher concentrations of the activator are used. At lower concentrations of the activator, CFB concretes with GGBFS show higher compressive strengths than the ones made with fly ash. This once again shows that the activator concentration has a greater influence on the compressive strength of CFB concretes with fly ash, which is confirmed using statistical analysis of the compressive strength results later in this section. While compressive strengths of the CFB concretes with fly ash rely solely on the formation of sodium aluminosilicate gel, for CFB concretes with GGBFS, some calcium bearing compounds also could be forming even at lower activator concentrations. This could be a reason for their increased strengths at lower activator concentrations as compared to CFB concretes containing fly ash. Microstructural analysis of pastes made with

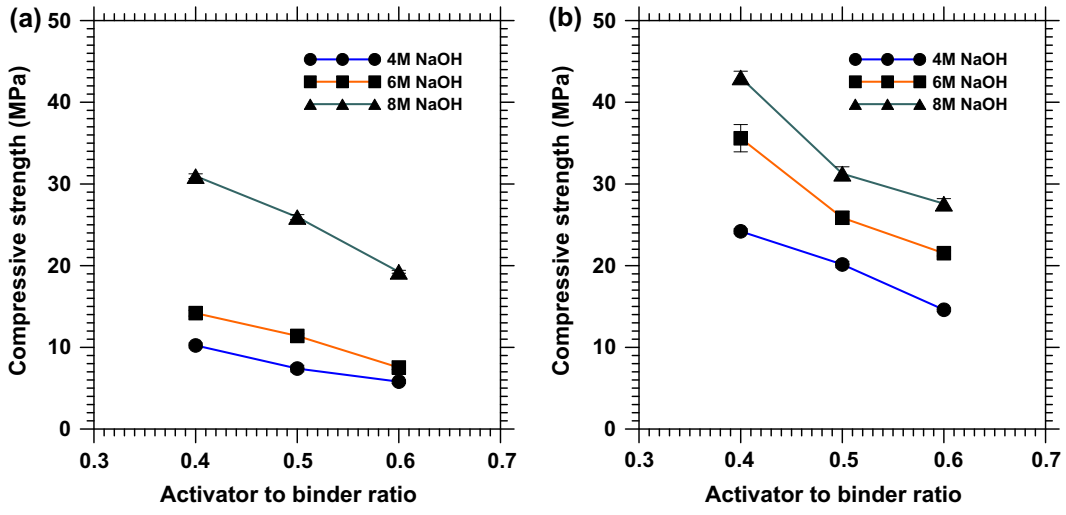

Fig. 6. Compressive strengths of CFB concretes as a function of activator-to-binder ratio: (a) fly ash as the starting material, and (b) GGBFS as the starting material.

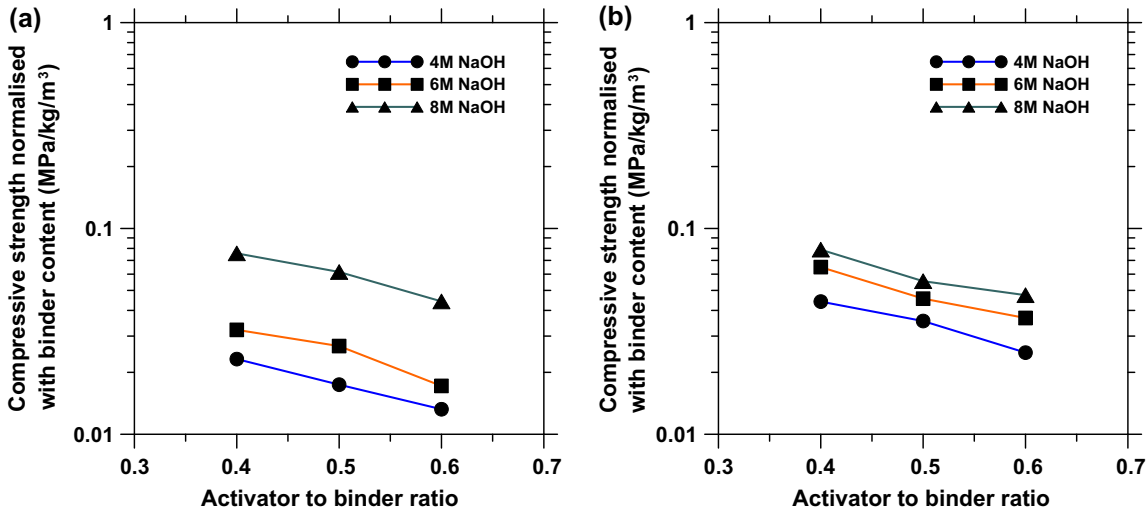

Fig. 7. Normalized compressive strengths of CFB concretes as a function of activator-to-binder ratio: (a) fly ash as the starting material, and (b) GGBFS as the starting material.

lower and higher activator concentrations is dealt with in a forthcoming section.

In order to obtain a better understanding of the influence of two factors – activator concentration (a) and activator-to-binder ratio (b) – on the compressive strength (f'_c), a 3^2 full factorial analysis was carried out with each factor at three levels. The levels of activator concentration (a) chosen were 4 M, 6 M, 8 M, and the levels for the activator-to-binder ratio (b) chosen were 0.40, 0.50, and 0.60. A quadratic model was found to better represent the compressive strengths of CFB concretes. Analysis of variance was carried out to facilitate elimination of the parameter combination(s) in the model that do not significantly influence the compressive strengths. The quadratic equations obtained from the factorial analysis for the compressive strengths of CFB concretes made with fly ash and GGBFS, respectively are given in Eqs. (1) and (2), and the corresponding three-dimensional response surfaces are shown in Fig. 8a and b.

$$f'_{c\text{fly ash}} = 26.4 - 7.7a + 16.5b - 9.0ab + 1.3a^2 \quad (1)$$

$$f'_{c\text{GGBFS}} = 65.0 + 7.2a - 221.7b - 7.3ab = 200.5b^2 \quad (2)$$

In these equations, the values of f'_c are in MPa, and the activator concentration in mol/l. A closer look at the above equations show that the square of the activator-to-binder ratio (b) does not have an influence on the compressive strengths of CFB concretes made using fly ash, but is influential for CFB concretes made using GGBFS. Similarly the square of the activator concentration (a) does not influence the strengths of CFB concretes made using GGBFS but influences the strength of CFB concretes made using fly ash. The accuracy of the developed models was confirmed from the normal probability plots of residuals, which fell on a straight line.

3.3. Pore structure of CFB concretes and pastes

3.3.1. Porosities of CFB concretes

Fig. 9a and b shows the porosities of CFB concretes made using fly ash or GGBFS as the starting materials as functions of the activator–binder ratio, at various activator concentrations. The porosities of CFB concretes were determined using a vacuum saturation method as explained in earlier.

From Fig. 9a and b, it can be observed that the porosities of CFB concretes increase with increase in the activator-to-binder ratio as expected. This is in agreement with the compressive strength results detailed earlier, which were shown to decrease with increase in activator-to-binder ratio. From Fig. 9a, it can be seen that the CFB concretes made using fly ash and activated using 4 M NaOH exhibits the highest porosity values. The porosity decreases with increase in activator concentration, attributable to the better activation efficiency and formation of increased amounts of reaction products. Similar trends are also observed in Fig. 9b for CFB concretes made using GGBFS. The porosities of CFB concretes made using GGBFS are found to be lower than those of CFB concretes with fly ash. The activator concentration is found to have a lesser influence on the porosity of CFB concretes made using GGBFS as compared to CFB concretes made using fly ash. This is in agreement with the trends for compressive strength also.

The relationship between compressive strengths and porosities for all the CFB concretes (made using either fly ash or GGBFS as the binder, and with varying activator concentrations and activator-to-binder ratios) is shown in Fig. 10. The porosity values ranged from 7% to 16%. The compressive strength–porosity relationship shows an exponential trend, similar to that of conventional concretes. For lower strength CFB concretes (<15 MPa), the trend seems to deviate from that of the mixtures having a higher compressive strength.

A 3^2 factorial analysis was carried out to model the influence of activator concentration (a) and activator-to-binder ratio (b) on the porosity of CFB concretes made using fly ash or GGBFS. Based on the analysis of variance tests, it was found that a linear model suffices to represent porosity (%) as a function of activator concentration (mol/l) and activator-to-binder ratio. These relationships are provided in Eqs. (3) and (4) for CFB concretes made using fly ash and GGBFS respectively. The adequacy of the model was ascertained from the normal probability plot of the residuals. Inspection of the coefficients for the variables in Eqs. (3) and (4) suggest that the activator-to-binder ratio (b) exerts significant influence on the porosity of the CFB concretes, especially at higher activator concentrations (a).

$$\phi_{FA}(\%) = 5.3 - 0.8a + 25.7b \quad (3)$$

$$\phi_{\text{GGBFS}}(\%) = 2.8 - 0.4a + 21.9b \quad (4)$$

3.3.2. Porosities and pore sizes of CFB pastes

The porosities of CFB pastes were determined using a vacuum saturation method as well as using image analysis procedures on

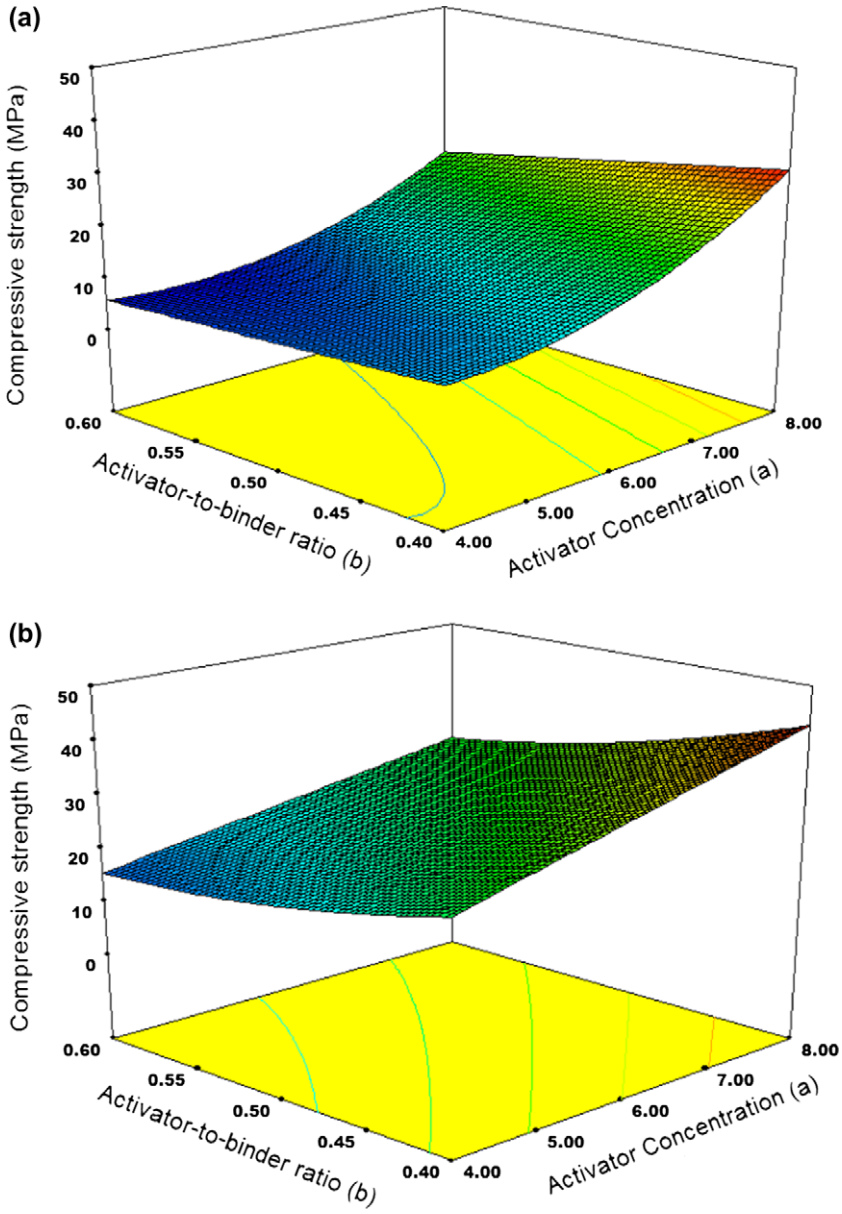

Fig. 8. Response surfaces showing the influence of activator-to-binder ratios and activator concentrations on the compressive strengths of CFB concretes made with: (a) fly ash, and (b) GGBFS as the starting materials.

polished sections. The porosities and pore sizes were investigated only for those GGBFS and fly ash CFB pastes made using activator-to-binder ratios of 0.40 and 0.60, and an activator concentration of 8 M. Fig. 11a shows the porosity (using vacuum saturation method) of CFB pastes made using fly ash or GGBFS as the starting material. The porosities of CFB pastes made using GGBFS are seen to be lower than for those made with fly ash; a trend that was observed for concretes also. The porosities of CFB concretes made using similar activator-to-binder ratios and activator concentration are shown as symbols along with bars for the porosities of the paste in Fig. 11a. The porosities of the CFB pastes are about three times more than those of concrete, because in CFB concretes, the paste volume is only about a third of the total volume.

The porosities of the CFB pastes obtained using the image analysis procedure is presented in Fig. 11b. The results are averages from 10 images corresponding to each specimen and the error bars represent one standard deviation from the mean value. Similar trends are observed between the paste porosities obtained either using vacuum saturation method or image analysis method. However the porosities obtained using image analysis method are only about half of the porosities obtained from the vacuum saturation method. This is because the image analysis method captures only those pores of size equal to or larger than 10 μm (because of the magnification used). However it can be safely stated from these results that about half of the total pore volume in CFB pastes made with either fly ash or GGBFS as the starting material is contributed by pores of size less than 10 μm. The distribution of pore sizes could be an influential parameter in the moisture and ionic transport in alkali-activated concretes.

Fig. 12 shows the characteristic pore size (pore size corresponding to 50% of the cumulative frequency distribution plot) in CFB pastes made using fly ash or GGBFS. The d_{50} values as represented here correspond to the characteristic value of pore sizes for pores greater than 10 μm ($d_{50(>10\ \mu m)}$). Thus these values should not be regarded as true indicators of the actual pore sizes in the material.

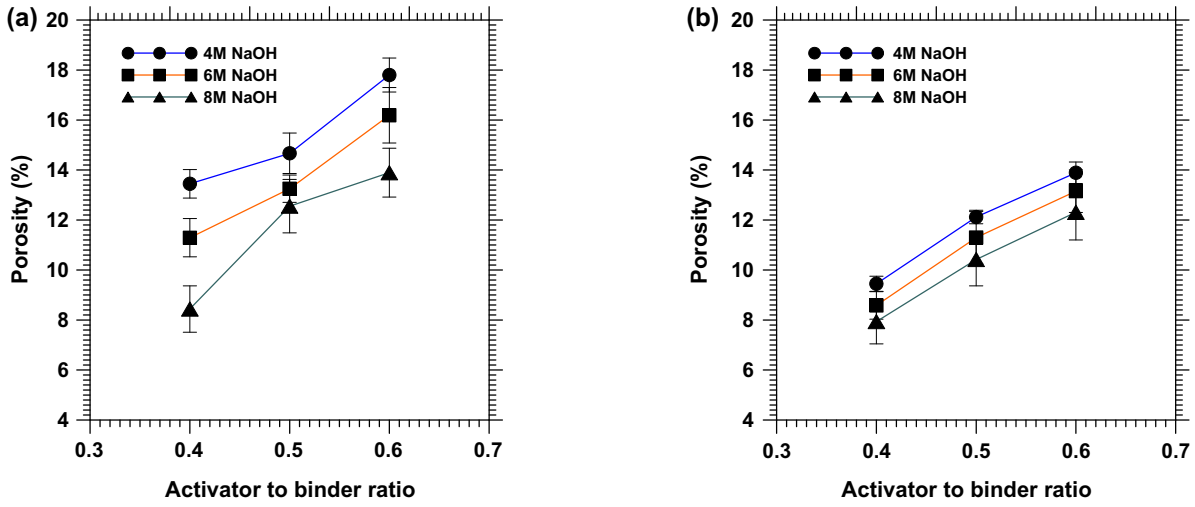

Fig. 9. Porosities (measured by vacuum saturation method) of CFB concretes made using: (a) fly ash, and (b) GGBFS as the starting material.

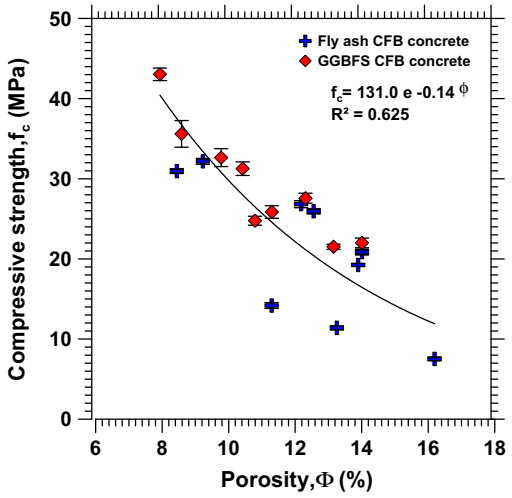

Fig. 10. Compressive strength–porosity relationship for CFB concretes.

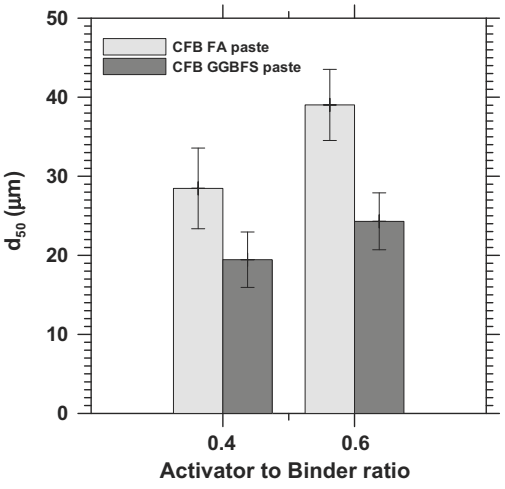

Fig. 12. Characteristic pore sizes ($d_{50(>10\ \mu m)}$) of CFB pastes.

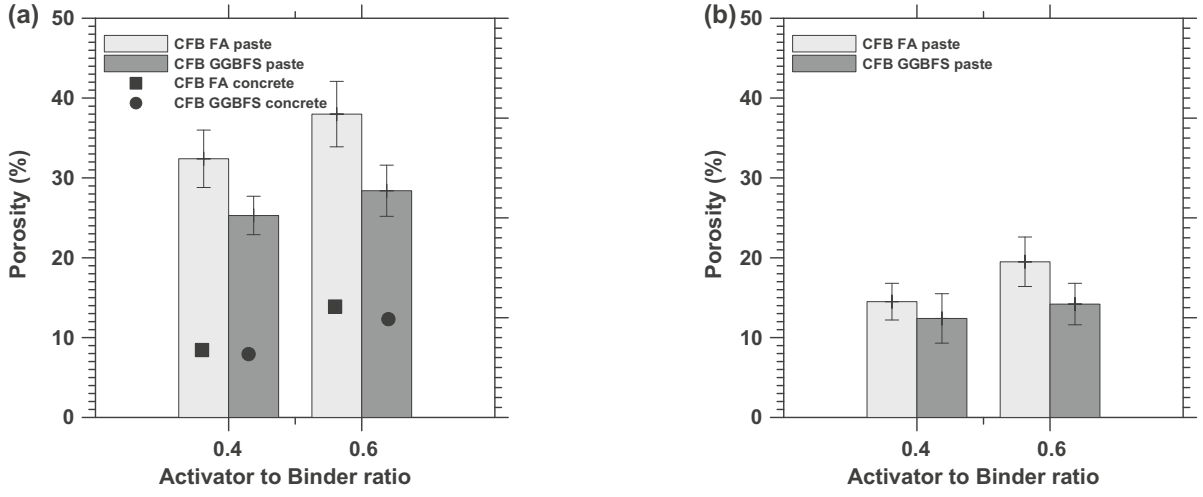

Fig. 11. (a) Porosity of CFB pastes and concretes measured by vacuum saturation method, and (b) porosities of CFB pastes obtained from image analysis method.

However this facilitates a comparison between the pore sizes in CFB pastes made using fly ash or GGBFS, and the influence of activator-to-binder ratio. The characteristic pore size of CFB pastes with fly ash is seen to be higher than those with GGBFS as the binder. The higher porosity and larger pore sizes in CFB pastes made using fly ash as compared to those made using GGBFS also provide a reason for the difference in compressive strengths of activated concretes when these starting materials are used.

3.4. Microstructure of CFB pastes

3.4.1. CFB pastes made from fly ash

Scanning electron microscopy (SEM) was used to understand the morphology of the reaction products in CFB pastes, while XRD was used for phase identification. Fig. 13a shows the micrograph of CFB paste made using fly ash as the starting material and activated using 4 M NaOH, while Fig. 13b shows the microstructure of the resultant paste when activated using 8 M NaOH. The activator-to-binder ratio in both these cases is 0.40. It can be seen that the paste obtained by activation using a lower concentration of the activator (4 M NaOH) shows more unreacted fly ash particles as compared to the paste obtained from activation using a higher concentration of the activator (8 M NaOH). This is evidence of increased gel formation when higher activator concentrations are used, which can also be related to the compressive strength results discussed earlier. It is seen that the reaction product forms a shell around the unreacted fly ash particles, which is particularly well observed in systems activated by a higher alkali concentration

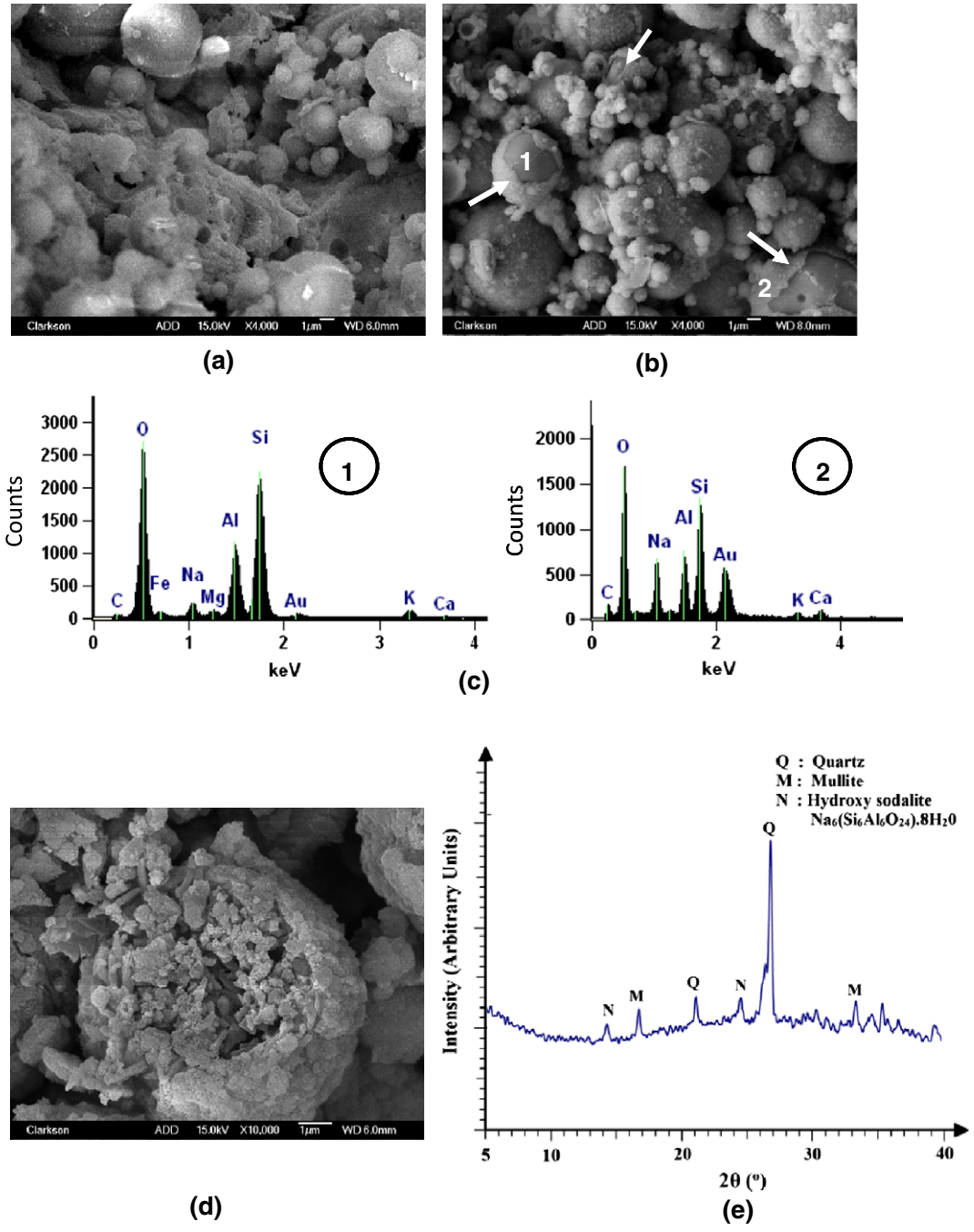

Fig. 13. (a) and (b) Micrographs of fly ash CFB pastes activated using 4 M and 8 M NaOH, respectively, (c) EDX at two locations shown in (b), (d) micrograph at higher magnification for paste activated using 8 M NaOH, and (e) XRD of paste activated using 8 M NaOH.

such as the one shown in Fig. 13b. NaOH dissolves the soluble phases in fly ash thereby releasing alumina and silica from the surface of fly ash particles. These phases then react with the alkalis from activating agent and condense on the surface of fly ash forming the aluminosilicate gel shell [32,33] shown by the arrows in Fig. 13b.

A significant amount of unreacted fly ash particles (the core on which the reaction products are precipitated) indicates that the degree of reaction is only low to moderate. Even when a higher concentration of activating alkali (such as 8 M NaOH) is used, there is likely a formation of a relatively thin layer of the reaction products on the surface of fly ash particle inhibiting its further activation (as can be seen in Fig. 13b). Though a large concentration of OH^- is available in the system at higher NaOH concentrations, the rate of further crystal growth would be slower if the fly ash particles are completely encapsulated by the aluminosilicate gel. Further activation is then controlled by diffusion as well as the pH gradients along the thickness of the reaction product around the unreacted fly ash core. Thus it is anticipated that even at further higher concentrations of the activating agent, the fly ash particles might not be completely utilized for the production of the reaction product, and the degree of reaction of the system might remain moderate.

The energy dispersive X-ray spectra (EDX) corresponding to the points marked "1" and "2" in Fig. 13b are shown in Fig. 13c. The

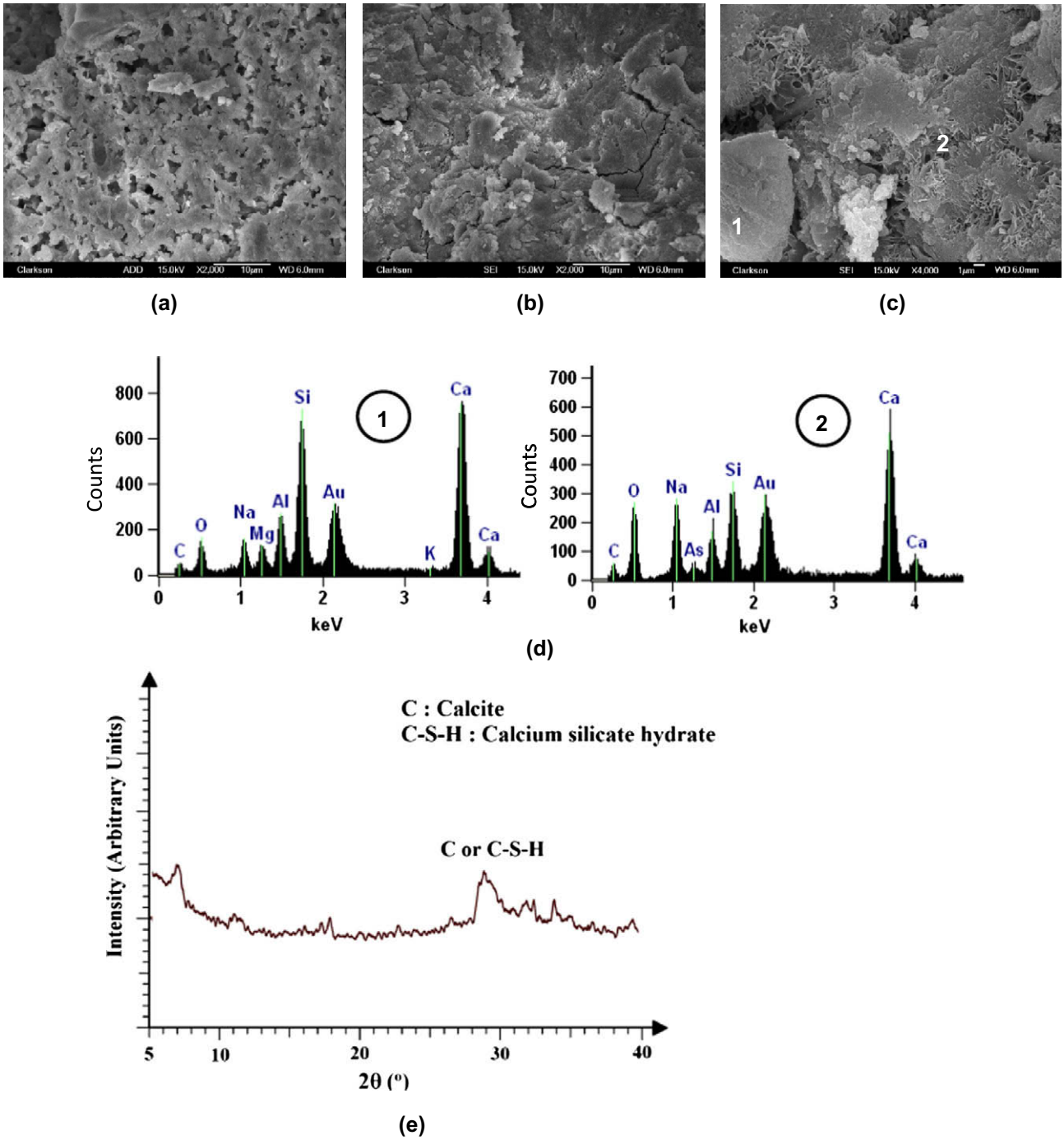

Fig. 14. (a) and (b) Micrographs of GGBFS CFB pastes activated using 4 M and 8 M NaOH, respectively, (c) micrograph at higher magnification for paste activated using 8 M NaOH, (d) EDX at two locations shown in (c), and (e) XRD of paste activated using 8 M NaOH.

EDX for point "1" is that of the unreacted core in a fly ash particle, whereas the EDX for point "2" shows the elemental composition of the reaction product. The Na to Al ratio of the Point "1" was determined to be 0.15, and that of Point "2" 0.83, indicating the higher Na content in the reaction product. The Si to Al ratio for the reaction product (Point "2"), determined from quantitative EDX was found to be approximately 2.0, which is in the range of reported values (1.8–2.0) for the aluminosilicate gel produced by the activation of fly ash using NaOH [22]. Fig. 13d shows a magnified view of a partly reacted fly ash plerosphere in a paste activated with 8 M NaOH that has retained its original shape. The activation process is seen to have resulted in the formation of the aluminosilicate gel outside the larger particle as well dissociation of the smaller spheres inside, forming more reaction products. A few randomly oriented and platey crystals, plausibly of hydroxy sodalite, are found in this micrograph.

Fig. 13e shows a typical XRD pattern of CFB pastes made fly ash as the starting material and 8 M NaOH as the activator. The XRD spectrum shows that the characteristic peaks of quartz and mullite remain even after alkaline activation with 8 M NaOH and heat treatment for 48 h. This shows the relatively low reactivity of these phases in alkaline conditions. Only the glassy phases in fly ash are the source of Al and Si to form the aluminosilicate gel. However a previous study [33] has shown that the quartz and mullite phases dissolve completely when very high activator solution-to-fly ash ratios (~3 to 6) are used. Such high ratios, commonly used for zeolite synthesis from precursor materials, cannot be typically used for concretes because of the adverse impact of higher amount of water in the activating solution on the compressive strengths and porosities. Lower alkaline solution-to-fly ash ratios such as the ones used here reduce the rate of crystal growth, and consequently reduce the formation of crystalline phases. In the case of low alkaline solution-to-fly ash ratios, a reaction product is quickly formed that engulfs the fly ash particle as shown in the micrographs discussed above, slowing down further activation of the fly ash particles, and thus resulting in only low to moderate degrees of reaction. The only crystalline aluminosilicate phase that is detectable in the XRD spectrum is that of hydroxy sodalite ($Na_6(-Si_6Al_6O_{24})\cdot 8H_2O$), which is a zeolite. Other crystalline aluminosilicate phases such as Na-phillipsite have been reported [33] at high activating solution-to-fly ash ratios, longer activating durations, and higher activating temperatures than those used in this study.

3.4.2. CFB pastes made from GGBFS

Fig. 14a shows the micrograph of CFB paste made using GGBFS as the starting material and activated using 4 M NaOH, and Fig. 14b corresponds to CFB paste activated using 8 M NaOH. The activator-to-binder ratio was 0.40 for both these pastes. Individual GGBFS particles cannot be isolated in these micrographs. The reaction product formed is much more compact, homogeneous, and uniform when compared to the pastes with fly ash as the starting material. A lower concentration (4 M NaOH) of the activator is found to create a microstructure that is more porous than that in a paste made using a higher (8 M NaOH) activator concentration (Fig. 14b). This shows that the use of a more concentrated alkali increases the amounts of reaction product formation, and consequently reduces the porosities, and increases the compressive strengths.

Fig. 14c is a micrograph at higher magnification of the CFB paste made using GGBFS activated with 8 M NaOH. The EDX spectra at two points marked "1" and "2" in Fig. 14c are shown in Fig. 14d. The EDX spectrum of the Point "1" shows that it is likely a GGBFS particle with some reaction products on the surface. In the matrix of reaction products, a few areas showing network of fibrous or flaky structures are apparent (Point "2"), plausibly C–S–H gel, which is stated as the main hydration product in alkali-activated slag cements [34]. The higher Ca to Si ratio (~1.4) at this point lends credence to this premise. The Na to Al ratio for the reaction product is rather high (~1.37) as compared to that in the reaction product of activated fly ash paste (~0.80), which could be attributable to the lower amounts of alumina in GGBFS. The EDX spectra for CFB pastes containing GGBFS are found to be significantly different both in the peak intensities and in composition (especially the presence of calcium) from those containing fly ash, showing that the reaction products formed from both these starting materials are different in structure and composition.

The XRD pattern for the CFB paste with GGBFS as the binder is shown in Fig. 14e. The paste is more amorphous than the reaction product of fly ash activation. At a 2θ angle of 29°, a peak that could be attributed to either calcite or C–S–H is observed. Occurrence of calcite can be attributed to the fact that carbonation is likely to occur during the mixing of very high amounts of alkalis to a binder that contains significant amounts of calcium oxide [35]. The presence of calcite at very early ages could be the cause of premature stiffening of CFB paste made with GGBFS which was observed during the time of mixing. No sodalite peaks are observed in the CFB paste with GGBFS, as was observed in the case of CFB paste with fly ash.

4. Conclusions

This paper has provided extensive experimental results and analysis on the compressive strengths, porosities, and microstructure of cement-free binder (CFB) pastes and/or concretes containing either fly ash or GGBFS as the sole binder and activated using NaOH solutions of different concentrations. The following conclusions are made based on this study:

1. The curing temperature was found to have a profound influence on the compressive strengths of CFB concretes containing fly ash as compared to those containing GGBFS. A curing temperature of 75 °C and a curing duration of 48 h resulted in maximum compressive strengths of the CFB concretes. CFB concretes with fly ash showed lower compressive strengths when heat cured at 60 °C irrespective of curing duration whereas CFB concretes with GGBFS showed reasonable compressive strengths even at lower curing temperatures.
2. Compressive strengths of CFB concretes were found to increase with increase in activator concentration and decrease in activator-to-binder ratio. The CFB concretes made using GGBFS as the starting material showed higher compressive strengths compared to those made with fly ash because of the self-cementing property of GGBFS and higher binder content used. When the compressive strengths were normalized with fly ash or GGBFS content, it was observed that the CFB concretes made using GGBFS and fly ash had similar compressive strength when activated using higher concentration of the activator. At lower concentrations of the activator, CFB concretes with GGBFS showed higher compressive strengths. A 3^2 factorial analysis and the quadratic equations for the response surface for compressive strengths showed that the activator concentration influences the compressive strengths of CFB concretes made using fly ash to a greater degree, whereas the activator-to-binder ratio exerts more influence on the compressive strengths of CFB concretes made using GGBFS.
3. Porosities of CFB concretes were found to decrease with increase in activating agent concentration and activator-to-binder ratio. The strength–porosity relationships for CFB concretes were also found to be exponential, similar to those for normal concretes. Statistical analysis showed that a linear relationship

adequately describes the influence of activator concentration and activator-to-binder ratio on porosities of CFB concretes. The porosities of CFB pastes were found to be about three times higher than those of CFB concretes, mainly because the paste volume is only about a third of the concrete volume. The characteristic size of pores larger than 10 μm ($d_{50(>10\ \mu m)}$) in CFB pastes was found to be higher for the paste made using fly ash as the starting material.

4. Microstructural observations revealed the formation of alkali-aluminosilicate gel as a shell around the fly ash particles whereas the reaction product was more homogeneously distributed in pastes made using GGBFS. The reaction product shell formed around the fly ash inhibits further activation, resulting in incomplete utilization of the fly ash particles. The presence of the crystalline phases of fly ash in the XRD pattern of the paste shows that only glassy phases in fly ash take part in gel formation. Hydroxy sodalite was the only crystalline aluminosilicate phase detected in CFB pastes with fly ash. The reaction product in the GGBFS paste showed the presence of significant amounts of calcium, in addition to the sodium, alumina and silica phases. The XRD pattern for the CFB paste made using GGBFS was mostly amorphous. The micrographs and the XRD patterns provide an insight into the differences in the reaction product morphology and composition when fly ash or GGBFS are used as the starting material in CFB concretes or pastes.

Acknowledgements

This study was partly funded by the Green and Energy Efficient Building Products and Systems program of the New York State Energy Research and Development Authority (NYSERDA). The materials for this study were provided by Holcim Cement and Graymont Materials. A part of the experimental study was carried out at the facilities of the Center for Advanced Materials Processing (CAMP) at Clarkson University. The authors acknowledge all these entities for the support.

References

[1] Palomo A, de la Fuente JIL. Alkali-activated cementitious materials: alternative matrices for the immobilization of hazardous wastes. Part I. Stabilization of boron. Cem Concr Res 2003;33:281–8.
[2] Davidovits J. Geopolymers: inorganic polymeric new materials. J Therm Anal 1991;37:1633–56.
[3] van Deventer JSJ, Provis JL, Duxson P, Lukey GC. Reaction mechanism in geopolymeric conversion of inorganic waste to useful products. J Hazard Mater 2007;139:506–13.
[4] Yunsheng Z, Wei S, Qianli C, Lin C. Synthesis and heavy metal immobilization behavior of slag geopolymer. J Hazard Mater 2007;143:206–13.
[5] Sun W, Zhang YS, Lin W, Liu ZY. In situ monitoring of the hydration process of K-PS geopolymer cement with ESEM. Cem Concr Res 2004;34:935–40.
[6] Wang H, Li H, Yan F. Synthesis and mechanical properties of metakaolinite-based geopolymer. Coll Surf A: Physicochem Eng Aspects 2005;268:1–6.
[7] Sofi M, van Deventer JSJ, Mendis PA, Lukey GC. Engineering properties of inorganic polymer concretes (IPCs). Cem Concr Res 2007;37:251–7.
[8] Rahier H, Van mele S, Wastiels J. Low-temperature synthesized aluminosilicate glasses. Part II. Rheological transformations during low-temperature cure and high-temperature properties of a model compound. J Mater Sci 1996;31:80–5.
[9] Alvarez-Ayuso E, Querol X, Plana F, Alastuey A, Moreno N, Izquierdo M, et al. Environmental, physical and structural characterization of geopolymer matrixes synthesized from coal (co-)combustion fly ashes. J Hazard Mater 2008;154:175–83.
[10] Duxson P, Provis JL, Luckey GC, Mallicoat SW, Kriven WM, van Deventer JSJ. Understanding the relationship between geopolymer composition, microstructure and mechanical properties. J Coll surf A: Physiochem Eng Aspects 2005;269:47–58.
[11] Bakharev T. Resistance of geopolymer materials to acid attack. Cem Concr Res 2005;35:658–70.
[12] Bakharev T. Durability of geopolymer materials in sodium and magnesium sulfate solutions. Cem Concr Res 2005;35:1233–46.
[13] Kong DLY, Sanjayan JG. Damage behavior of geopolymer composites exposed to elevated temperatures. Cem Concr Compos 2008;30:986–91.
[14] Criado M, Fernández-Jiménez A, de la Torre A, Aranda MAG, Palomo A. An XRD study of the effect of SiO_2/Na_2O ratio on the alkali activation of fly ash. Cem Concr Res 2007;37:671–9.
[15] van Jaarsveld JGS, van Deventer JSJ, Lukey G. The characterization of source materials in fly ash-based geopolymers. Mater Lett 2003;57:1272–80.
[16] Silva PD, Crenstil KS, Sirivivatnanon V. Kinetics of geopolymerization: role of Al_2O_3 and SiO_2. Cem Concr Res 2007;37:512–8.
[17] Temuujin J, van Riessen A, Williams R. Influence of calcium compounds on the mechanical properties of fly ash geopolymer pastes. J Hazard Mater 2009. doi:10.1016/j.jhazmat.2008.12.12.
[18] Hardjito D, Rangan BV. Development and properties of low-calcium fly ash-based geopolymer concrete. Curtin research report. <http://www.geopolymer.org/library/technical-papers/17-development-and-properties-of-low-calcium-fly-ash-based-geopolymer-concrete>.
[19] Yang KH, Song JK, Ashour AF, Lee ET. Properties of cementless mortars activated by sodium silicate. Constr Build Mater 2009;22:1981–9.
[20] Sathonsaowaphak A, Chindaprasirt P, Pimraksa K. Workability and strength of lignite bottom ash geopolymer mortar. J Hazard Mater 2009. doi:10.1016/j.jhazmat.2009.01.12.
[21] Shi C. Strength, pore structure and permeability of alkali-activated slag mortars. Cem Concr Res 1996;26:1789–99.
[22] Fernández-Jiménez A, Palomo A, Criado M. Microstructure development of alkali-activated fly ash cement: a descriptive model. Cem Concr Res 2005;35:1204–9.
[23] Xu H, van Deventer JSJ. The geopolymerization of alumino-silicate minerals. Int J Miner Process 2000;59:247–66.
[24] Davidovits J. Geopolymer chemistry and sustainable development. The Poly(sialate) terminology: a very useful and simple model for the promotion and understanding of green-chemistry. In: Davidovits J, editor. Proceedings of the world congress geopolymer, Saint Quentin, France; 2005. p. 69–73.
[25] Mozgawa W, Deja J. Spectroscopic studies of alkaline activated slag Geopolymers. J Mol Struct 2009. doi:10.1016/j.molstruct.2008.12.026, 200.
[26] Bakharev T. Geopolymeric materials prepared using Class F fly ash and elevated temperature curing. Cem Concr Res 2005;35:1224–32.
[27] Chindaprasirt P, Chareerat T, Sirivivatnanon V. Workability and strength of coarse high calcium fly ash geopolymer. Cem Concr Compos 2007;29:224–9.
[28] Provis JL, van Deventer JSJ. Geopolymerisation kinetics. 2. Reaction kinetic modeling. Chem Eng Sci 2007;62:2318–29.
[29] Panias D, Giannopouloua IP, Perraki T. Effect of synthesis parameters on the mechanical properties of fly ash-based geopolymer. J Coll Surf A: Physicochem Eng Aspects 2007;301:246–54.
[30] RILEM CPC11.3. Absorption of water by immersion under vacuum. Mater Struct 1984;17:391–4.
[31] Kovalchuk G, Jimenez AF, Palomo A. Alkali-activated fly ash: effect of thermal curing conditions on mechanical and microstructural development – Part II. Fuel 2007;86:315–22.
[32] Fernández-Jiménez A, Criado M. Microstructure development of alkali-activated fly ash cement: a descriptive model. Cem Concr Res 2004;35:1204–9.
[33] Rios CAR, Williams CD, Roberts CL. A comparative study of two methods for the synthesis of fly ash-based sodium and potassium types zeolite. Fuel 2009;88:1403–16.
[34] Taylor HFW. Cement chemistry. 2nd ed. London: Thomas Telford; 1997.
[35] Astutiningsih S, Liu Y. Geopolymerisation of Australian slag with effective dissolution by the alkali. In: Davidovits J, editor. Proceedings of the world congress geopolymer, Saint Quentin, France; 2005, p. 69–73.